Progress In Electromagnetics Research M, Vol. 118, 117–126, 2023

Characterization of the Shielding Effectiveness of Composite Materials Using Electromagnetic Methods Covering a Wide Frequency Range

Rassoul Mansour*, Nabil Benjelloun, and Moncef Kadi

Abstract—Composite materials are being widely used in the automotive industry where they are progressively replacing metallic materials as structural parts for being robust and lightweight. Their complexity, often leading to lots of unknown behavioral effects when placed near the electronic systems present in vehicles, should be studied and treated. In the automotive industry, the shielding effectiveness of these materials should be considered as the most important parameter to be known in advance. Faurecia, one of the world's largest leading automotive suppliers, sought to assess the shielding effectiveness of their product such as dashboards and door trims. Their objective was to enhance the shielding effectiveness, thereby ensuring superior isolation and protection of electronic systems against electromagnetic interferences (EMI). Thus, this paper presents a novel method for characterizing the shielding effectiveness of various composites using two electromagnetic methods to cover a wide frequency range, starting from 10 Hz up to 8 GHz. The first method, based on loop antennas, was used to cover the low frequency range starting from 10 Hz up to 120 MHz. Frequencies between 100 kHz and 1.5 GHz were not discussed in this paper due to the numerous existing studies in this frequency range, using coaxial transmission cell. The second method, employed for frequencies higher than 1.5 GHz, consists of ultra-wideband antennas (Vivaldi).

1. INTRODUCTION

Composite materials are defined as the combination of two or more materials with different physical properties, which are not melted or mixed together, resulting in a complex composition. They consist of a reinforcement material and a matrix material. The former represents the skeleton of the composite because of its capability to withstand any applied mechanical effort. The latter, surrounding the former, acts as a binder and can give the desired shape to the material. Consequently, composites are heterogeneous mixtures of conductors and dielectrics that present a complex behavior challenging to study in the presence of electromagnetic fields.

Measuring reliable EMI Shielding Effectiveness data at a broad frequency range for different composite materials is crucial to determine their properties and potential applications. Several theoretical and experimental methods exist for measuring the shielding effectiveness. Regarding the theoretical methods, Schelkunoff [1] was the first to express the shielding effectiveness of a conductive plate as a function of its thickness, electrical conductivity, and impedance. Later on, subsequent models, like the Colaneri Model [2] and Poulichet Model [3], provided approximations and simplifications. These equations vary greatly between far field and near field measurements. In the near field, the incident plane wave is usually substituted either by a small electric dipole source for electric shielding measurements,

Received 5 June 2023, Accepted 4 August 2023, Scheduled 13 August 2023
* Corresponding author: Rassoul Mansour (rassoul.mansour@esigelec.fr).
The authors are with the Normandie Université, UNIROUEN, ESIGELEC, IRSEEM, Technopôle du Madrillet, Avenue Galilée, Saint-Etienne-du Rouvray 76801, France.

or by a small loop for magnetic shielding measurements. Studies have shown that the electric field is highly reflected by the conductive plate's surface, rendering the electric field inside the conductive plate negligible [4, 5]. However, this is not the case for the magnetic field. As a result, our study focuses on measuring the shielding effectiveness in terms of magnetic field attenuation to respect the needs of the automotive industry.

Furthermore, there is the Moser model [6] which is widely applied to measure the magnetic shielding effectiveness of conductive plates in the near field area.

If composite materials with square grid conductive fibers were to be studied, the cited models can only be applied at very low frequencies where the material behaves like a homogenized conductive plane, considering that the wavelength is much larger than the grids. At higher frequencies, Casey [7] developed a model suitable for such composites, which mainly depends on the diameter of the conductive fibers and the distance between them.

As for the experimental methods, shielding effectiveness (SE) can be mainly measured using closely spaced dipole antennas or a coaxial cable/cell. However, obtaining accurate SE measurements for extremely low frequencies, below 150 kHz, or for high frequencies, exceeding 1 GHz, present challenges [8]. Many SE measurement studies, employing coaxial transverse electromagnetic (TEM) cells, such as ASTM ES7-83 and D4935-89 standards, have primarily focused on the frequency range between 100 MHz and 1.5 GHz [9–14]. As a result, this frequency range will not be considered in our study. Consequently, the primary objective of this paper is to precisely characterize the shielding effectiveness of several composite plates using magnetic loops for the very low frequencies and ultra-wideband (UWB) Vivladi antennas for the high frequencies, thereby covering a wide frequency range from 10 Hz to 8 GHz. The experimental results will then be reproduced with the theoretical models in order to obtain the equivalent conductivity of a homogenous model of the shield.

This paper is organized as follows. Section 2 elaborates the different theoretical models that exist, essential for reproducing the experimental results. Section 3 presents the composition of ten different composites that we want to characterize. Section 4 features the experimental methods and setups which are based on the measurement of the ratio of the intensity of the incident electric/magnetic field to the intensity of the transmitted electric/magnetic field.

2. THEORETICAL MODELS

The shielding effectiveness is usually expressed in terms of losses: Reflection losses (R) on the material's surface, Absorption (A) in the material, and the multiple reflections within the material (MR). thus, the shielding effectiveness can be described by the following equation [11, 15]:

$$SE = A + R + MR \tag{1}$$

According to Schelkunoff [1], the absorption loss parameter, resulting from power converted to heat within the material, is highly dependent on the skin effect δ and the thickness d of the material under test. Thus, it is given by:

$$A = 20 \log \left(e^{\frac{(1+j)d}{\delta}} \right) \tag{2}$$

with

$$\delta = \frac{1}{\sqrt{\pi \mu f \sigma}} \tag{3}$$

where μ is the material's magnetic permeability, and σ stands for its electrical conductivity.

The absorption level is low at first but significantly increases with the frequency. With a thickness of 5δ, the signal is absorbed by 99% in the material. As for the reflection loss parameter, due to an electrical impedance variation between the free space and the material, the loss term can be expressed by:

$$R = 20 \log \frac{(Z_0 + Z_M)^2}{4 Z_0 Z_M} \tag{4}$$

where $Z_0 = \sqrt{\frac{\mu_0}{\varepsilon_0}} = 377\,\Omega$, the free space impedance and Z_M, for the material's impedance, as presented by:

$$Z_M = \sqrt{\frac{j\omega\mu}{\sigma + j\omega\varepsilon}} \tag{5}$$

The third and last parameter, expressed in (6), represents the multiple reflection loss parameter or sometimes referred as a correction factor. Generally, it is considered insignificant for thick conductive materials but can take negative values when the material is thin and poorly conducting [16].

$$MR = 20\log\left|1 - \frac{(Z_M - Z_0)^2}{(Z_M + Z_0)^2}\, e^{-2(1+j)\frac{d}{\delta}}\right| \tag{6}$$

In the near field area, the free space impedance should be substituted with an electric or magnetic wave impedance with a value other than 120π. MR then becomes dependent on the distance between the antenna and the test sample.

However, Moser in [6] represented the near-field shielding effectiveness with a different approach, as shown in (7):

$$SE_{mag} = 20\log\left|\frac{1}{4\mu_r}\frac{\displaystyle\int_0^\infty \left(\frac{\lambda^2}{\tau_0} J_1(\lambda a)\, e^{-\tau_0 b} d\lambda\right)}{\displaystyle\int_0^\infty \left(\frac{C\lambda^2\tau}{\tau_0^2} J_1(\lambda a)\, e^{-\tau_0 b - d(\tau-\tau_0)} d\lambda\right)}\right| \tag{7}$$

where,

$$C = \left[\left(\frac{\tau}{\tau_0} + \mu_r\right)^2 - \left(\frac{\tau}{\tau_0} - \mu_r\right)^2 e^{-2d\tau}\right]^{-1} \tag{8}$$

$$\tau = \sqrt{\lambda^2 - \gamma^2} \tag{9}$$

$$\tau_0 = \sqrt{\lambda^2 - \gamma_0^2} \tag{10}$$

$$\gamma = (j\omega\mu_0\mu_r\sigma)^{\frac{1}{2}} \tag{11}$$

$$\gamma_0 = j\frac{\omega}{c} \tag{12}$$

with J_1, the Bessel function of order 1, a, the loop radius, b, the distance between the loops, d, the shield's thickness, γ, the propagation constant in the shield, and γ_0, the free space propagation constant.

Regarding the measurement of the shielding effectiveness of square grid materials in the far field area, Casey's model considered the shield as not only resistive but also inductive. It is expressed by:

$$SE = -20\log\frac{2Z_s}{Z_0 + 2Z_s} \tag{13}$$

where,

$$Z_s = R_s + jL_s\omega \tag{14}$$

$$R_s = \frac{p}{\pi R^2\sigma_f}\frac{\sqrt{j\omega\tau}J_0\left(\sqrt{j\omega\tau}\right)}{2J_1\left(\sqrt{j\omega\tau}\right)} \tag{15}$$

$$\tau = \mu_0\sigma_f R^2 \tag{16}$$

$$L_s = \frac{\mu_0 p}{2\pi}\ln\left(1 - e^{\left(-2\pi\frac{R}{p}\right)}\right)^{-1} \tag{17}$$

with Z_s, the impedance of the grid, R_s, the resistance, L_s, the inductance, p, the distance between the conductive fibers, R, its radius, and σ_f, its conductivity.

As mentioned above, Casey envisioned the square grid composite as a material with a complex impedance, and not only a resistance, in which the imaginary part, the inductance, is frequency

dependent and progressively increases with frequency. This phenomenon is explained by the fact that at higher frequencies, the wavelength is comparable to the square gaps, leading to an improved transmission and consequently to a lower shielding effectiveness.

These models will be later used in our study to attempt to reproduce the experimental results and to obtain the homogenized electrical conductivity of the composite under test.

3. COMPOSITES COMPOSITION

Ten different composites (120 cm × 90 cm) were characterized. Fig. 1 displays a photo of one of the composite plates under study, with a thickness of 2.6 mm. Table 1 provides the thickness of these 10 composites.

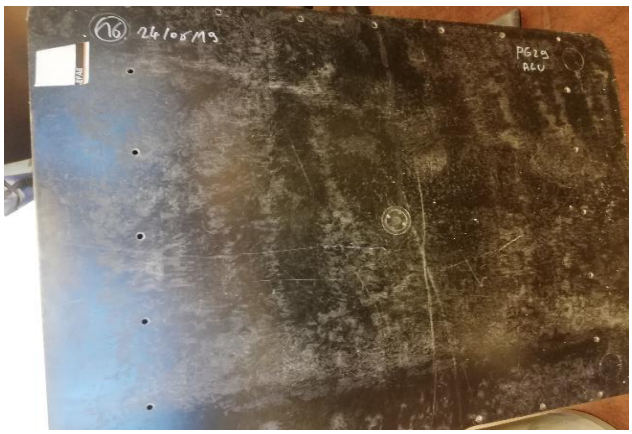

Figure 1. Photo of composite 1 (120 cm × 90 cm × 2.6 mm).

Table 1. The thickness of the different composites under test.

Composite	**1**	**2**	**3**	**4**	**5**	**6**	**7**	**8**	**9**	**10**
Thickness (mm)	2.6	5.0	2.8	3.1	2.6	2.6	3.0	2.6	2.6	2.6

Composites 1, 5, and 8 are composed of an aluminum grid, a steel grid, and a copper grid, respectively. Composites 3 and 4 represent two stacked steel grids and two stacked aluminum grids, respectively. Composites 2 and 9 consist of aluminum foil with copper tape. Composites 6 and 7 are made of short aluminum fibers compressed in the form of sheets on one side (composite 6) and on both sides (composite 7), respectively. Lastly, composite 10 represents a black steel grid.

4. EXPERIMENTAL METHODS

4.1. Magnetic Loops (10 Hz–120 MHz)

In order to determine the shielding effectiveness of composites plates at very low frequencies, the use of magnetic loops is inevitable. This method has been widely employed [6, 17, 18] for frequencies lower than 1 MHz, by measuring the attenuation of the magnetic fields by the shield, as shown in (18).

$$SE_H = 20 \log \left| \frac{H_i}{H_t} \right| \tag{18}$$

with H_i, the incident magnetic field and H_t, the transmitted magnetic field.

Therefore, we chose this as our first method and employed two pairs of magnetic loop antennas. The first pair covers the frequency range of 10 Hz–150 kHz (pair 1) while the second covers the frequency

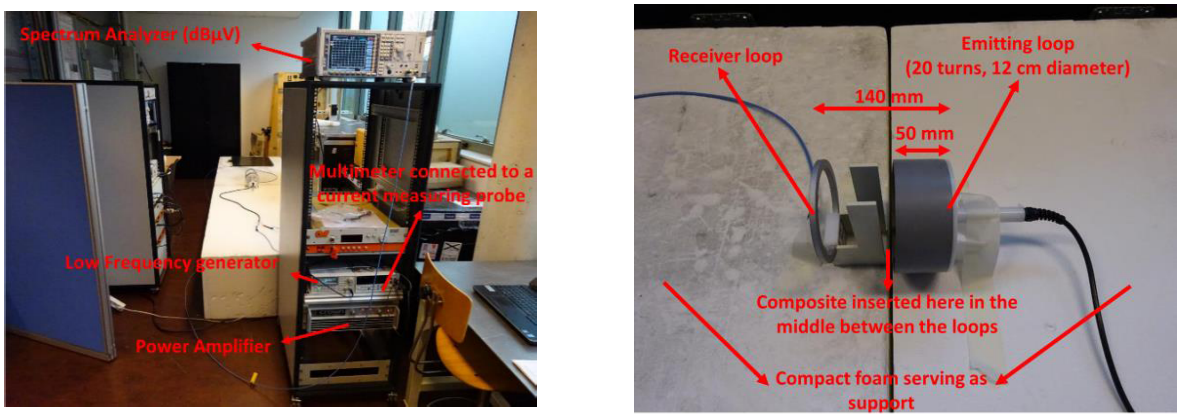

(a) (b)

Figure 2. (a) Experimental set-up used for the measurements of SE_H for the frequency range 10 Hz–150 kHz. (b) Photo of the two loops facing each other.

range of 100 kHz–120 MHz (pair 2). Fig. 2 presents the experimental setup of one of the two pairs. Despite the different working frequencies, nearly identical measurement protocols were applied to each pair. For the first pair, we used a low frequency generator, while for the second pair, a radiofrequency Synthesizer Rhode&Schwarz (9 kHz–2.08 GHz) was used. A signal amplifier (Crown macro-tech 5002VZ — Pair 1, and Amplifier Research 10W1000C — Pair 2) followed both generators, and its output was connected to the transmitting loops (Schwarzbeck FESP 5132 — Pair 1, Schwarzbeck HFRA 5164 — Pair 2).

A current probe is connected to the cable arriving at the emitting loop. The probe monitors the maximum current that the loop can handle. The pickup coils (Schwarzbeck FESP 5133-7/41 — Pair 1, Schwarzbeck FESP 5134-1 — Pair 2) were connected to a spectrum analyzer (Rhode & Schwarz ESU, 20 Hz–8 GHz — Pair 1, Rhode & Schwarz FSP, 9 kHz–7 GHz — Pair 2) to measure the magnetic field strength. Measurements were conducted at different frequencies. For each frequency, two measurements were taken: one in free space and the other with the shield inserted between the two coils. The difference between these two measurements gives us the value of the magnetic shielding effectiveness.

Results of pair 1 are depicted in Fig. 3. We note that the shielding is negligible at frequencies below 0.1 kHz for all the composites. Above 0.1 kHz, up to 150 kHz, we find that composite 2 has the best shielding, reaching a value of 60 dB at 150 kHz. This can be attributed to its greater thickness and its composition of excellent conductors: copper foil and aluminum foil. Composite 9 presents half the value of shielding obtained with composite 2 (30 dB at 150 kHz), due to its smaller thickness. We proceed by comparing the results of single grid composites. Composite 8 notably demonstrates the best shielding among the four grid composites with a value of 33 dB at 150 kHz, which is entirely expected given its composition of copper. Composite 1 follows with 26 dB at 150 kHz, followed by composite 10 (20 dB at 150 kHz) and 5 (7 dB at 150 kHz), as steel has lower conductivity than both copper and aluminum.

Additionally, we notice that composites with two grids, such as composites 3 and 4, present higher shielding values than those with a single grid. For instance, composite 4, comprising two aluminum grids, shows a shielding effectiveness that is 15 dB higher than composite 1, which consists of a single grid. A similar trend can be observed between composites 3 and 5, where composite 3, composed of two steel grids, has higher SE than composite 5, composed of a single steel grid. This phenomenon arises from the increase in the effective electrical conductivity when the material comprises two grids instead of one. Finally, both composites 6 and 7, formed of short aluminum fibers compressed as sheets on one side or both sides, respectively, exhibit negligible values of shielding, allowing the magnetic field to pass almost completely.

In order to determine the equivalent electrical conductivity of the tested composites, we tried to reproduce the curves using both the Schelkunoff and Moser models. Given that the conductivity varies with frequency, we manually reproduced the experimentally obtained SE values at 10 kHz and

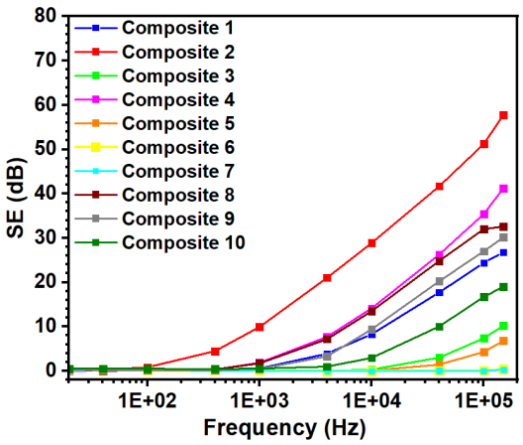

Figure 3. Measurements (Pair 1) of the magnetic shielding effectiveness as a function of frequency for 10 different plates.

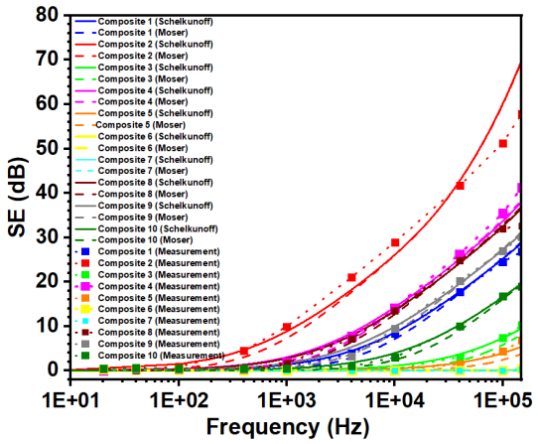

Figure 4. Fitting of the experimental data (Pair 1) by both Schelkunoff and Moser models for the magnetic shielding effectiveness.

at 100 kHz for each composite using a developed MATLAB algorithm. Therefore, we obtained four slightly different conductivity values for each plate. Subsequently, we calculated the average values, as shown in Table 2. These average values were then employed to recreate the curves using both models. Table 2 also gives an example of the values obtained for the Reflection (SER) and Absorption (SEA) losses at 100 kHz using Schelkunoff model. Fig. 4 displays the comparison between the models and the experimental data for some of the composites. The agreement between the theoretical and experimental data is evident, affirming the accuracy of the identified equivalent conductivity values.

Table 2. Values of the average electrical conductivities found using both Schelkunoff and Moser models along with the absorption (SEA) and reflection (SER) losses obtained with the Schelkunoff model at 100 kHz.

Composite	Electrical Conductivity (S/m)	SER at 100 kHz (dB)	SEA at 100 kHz (dB)
1	3.26×10^5	16.68	7.77
2	1.78×10^6	22.80	29.38
3	2.16×10^4	6.48	2.36
4	7.49×10^5	20.16	14.98
5	1.11×10^4	4.19	1.01
6	50	0.02	0.01
7	50	0.03	0.01
8	7.27×10^5	19.68	11.87
9	1.12×10^5	17.36	8.97
10	1.11×10^5	12.32	4.81

Results of the second pair covering the remaining frequency range are illustrated in Fig. 5. For each measurement, only twelve frequency points are taken into consideration because we had numerous plates to characterize. As we can see, composite 2 is absent because of its important losses that surpass the level of 90 dB, which does not respect the dynamic range (approximately 90 dB for a RBW of 9 kHz) of our spectrum analyzer. The shielding effectiveness of composites 1 and 4 continues to rise until it reaches a stable level of 38 dB and 50 dB, respectively. We notice that composite 4 (composed of two aluminum grids) maintains superior shielding compared to composite 1 (consisting of a single aluminum grid), consistent with the results shown in Fig. 3. Similarly, composite 8 reaches a stable level of around 41 dB, slightly surpassing that of composite 1, knowing that it is a copper grid with a conductivity

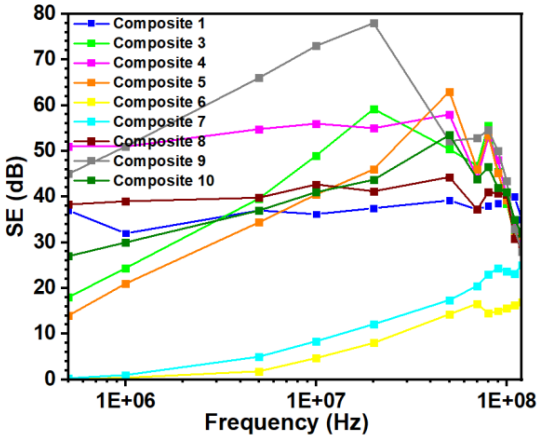

Figure 5. Measurements (Pair 2) of the shielding effectiveness as a function of frequency for the different composite plates.

higher than aluminum's. The shielding effectiveness of composites 3 (with two grids) and 5 (with one grid) made from steel grids increases with frequency, with the former displaying greater shielding. Both composites reach a cut-off frequency before experiencing a decline. The same behavior can be observed with composite 10, which is composed of a black steel grid. Although the results slightly differ due to the distinct steel type, the increase followed by the decrease in shielding is still evident. Interestingly, the results of these three steel grid composites resemble those of a conductive plate, like composite 9. This can be attributed to the fact that steel-based composites have a much smaller distance between the fibers p than copper or aluminum grid composites (composites 1, 4, and 8). A similar pattern is observed for the remaining composites 6 and 7 due of their comparable composition. Both composites show negligible SE up to 5 MHz and 1 MHz, respectively. Beyond these frequencies, a gradual increase in the shielding effectiveness is noticeable.

4.2. Ultra Wide Band Antennas (1.5 GHz–8 GHz)

Frequencies higher than 1 GHz and up to 8 GHz were covered using ultra-wideband antennas based on Vivaldi antennas. These antennas were positioned face to face at a distance of 18 cm within an anechoic cell, where the sample was inserted between the two antennas in the form of a sandwich. Both antennas were connected to a Vector Network Analyzer (Rhode & Schwarz) to measure the transmission parameter. Fig. 6 provides photos of the anechoic cell containing the positioned antennas connected to the Vector Network Analyzer (VNA).

In order to measure the shielding effectiveness, a measurement without a plate between the two antennas was conducted to evaluate the losses in free space. Consequently, the shielding effectiveness of various composite plates can be calculated using the formula:

$$SE = |S_{21\,composite}| - |S_{21\,free\,space}| \tag{19}$$

Figure 7(a) displays the variation of the transmission parameter as a function of frequency with a resolution bandwidth (RBW) of 10 Hz, aiming to achieve the best possible dynamic range (approximately 110 dB). Using (19), the shielding effectiveness SE for different composites was calculated, and the results are presented in Fig. 7(b). Two distinct types of curves are observed: the first type exhibits a decrease in SE with increasing frequencies, while the second type shows a slight increase. As previously discussed, grid composites are expected to improve transmission as frequency increases. As a result, the curves belonging to the first type primarily represent grid composites (composites 1, 4, 5, 8, 10), except for composite 3 where SE exceeds the dynamic range. The other composites demonstrate stability or even a slight increase in SE due to their composition, which categorizes them as more conductive plates.

The variation of SE among different grid composites depends on the diameter of the conductive fibers d and the distance p that separates them. For instance, composites 1 ($p = 1.45$ mm; $d = 360$ µm)

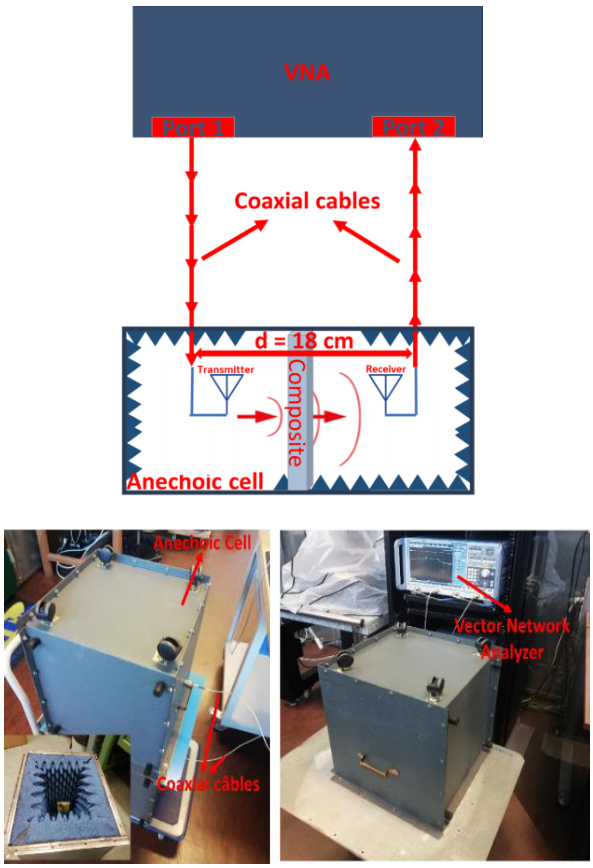

Figure 6. Experimental setup with the anechoic cell containing the Vivaldi antennas connected to the VNA.

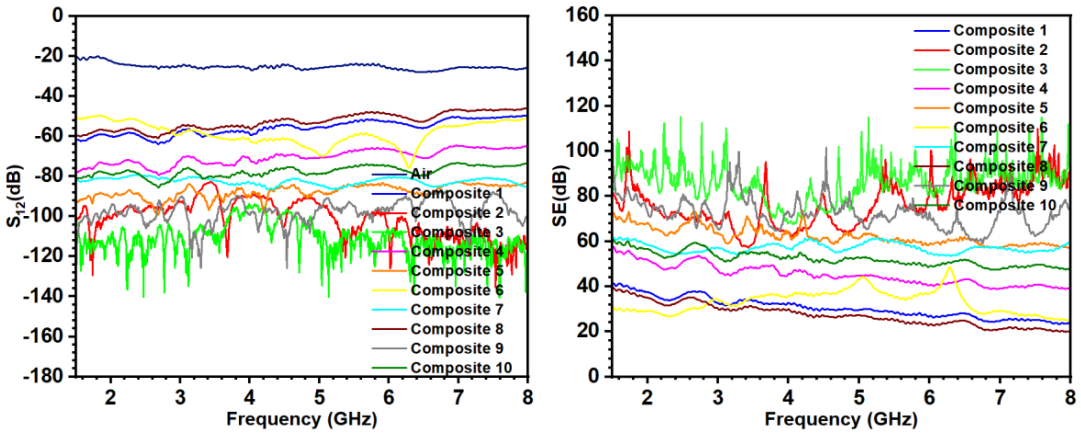

Figure 7. (a) Variation of the transmission parameter as a function of the frequency for 10 different composites. (b) Variation of the shielding effectiveness as a function of frequency for 10 different composites.

and 8 ($p = 1.476\,\text{mm}$; $d = 270\,\mu\text{m}$) yield similar SE, approximately 32 dB at 3 GHz, given their analogous properties. Conversely, composite 5, composed of steel ($p = 0.144\,\text{mm}$; $d = 110\,\mu\text{m}$), exhibits higher SE of around 64 dB at 3 GHz due to the considerably smaller distance between fibers p, rendering

it more compact and consequently more conductive. Composites 4 (50 dB at 3 GHz) and 3 (> 80 dB) yield higher SE than composites 1 and 5, respectively, owing to their composition of two stacked grids. Finally, composite 10, composed of black steel ($p = unknown$; $d = unknown$), presents a SE value of roughly 56 dB at 3 GHz.

We then attempted to reproduce the curves of single mesh composites using Casey's model, as shown in Fig. 8. We notice that the model fits exceptionally well, particularly for composites 1 and 8. However, composite 5 shows a slight difference of approximately 5 dB between the model and the measurement.

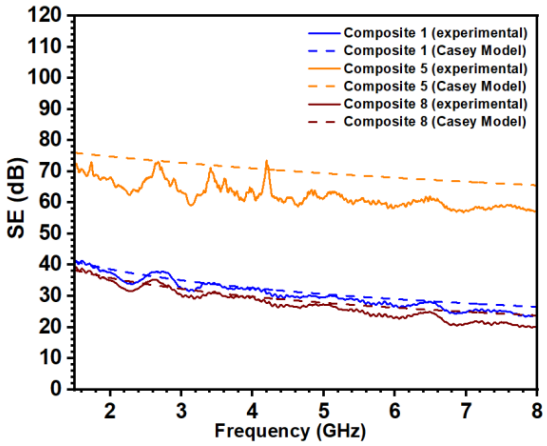

Figure 8. Fitting of the experimental data of composites 1, 5 and 8 by Casey model for the shielding effectiveness.

For the remaining non-grid composites, their SE values are influenced by the electrical conductivity of the constituent materials. It is evident that composites 2 and 9 exhibit higher SE values (> 70 dB) than composites 6 and 7 (32 dB and 68 dB at 3 GHz) due to the presence of copper tape in the first two, rendering them significantly more conductive.

5. CONCLUSION

In summary, this paper introduced various electromagnetic methods for measuring the shielding effectiveness of different composite materials. For low frequencies and up to 120 MHz, magnetic loops were employed. It was found that below 0.1 kHz, the signal was fully transmitted regardless of the composite's composition. Differences were observed afterwards as the shielding effectiveness of all composites began to exponentially increase with frequency before reaching a stable value. Composite 2 showed the highest shielding among all composites. For frequencies above 1.5 GHz, a pair of Vivaldi antennas was used. Results were separated into two groups: grid composites and plate composites. The former exhibited a decrease in the shielding effectiveness with frequency due to the decrease of the wavelength in comparison with the square gaps, leading to an improved transmission. In contrast, the latter demonstrated a slight increase attributed to the absorption phenomenon. These different methods effectively covered the entire frequency range from 10 Hz to 8 GHz, making them suitable for application in the automotive industry. These innovative methods can be utilized for any composite, regardless of thickness or composition.

ACKNOWLEDGMENT

The authors would like to acknowledge Faurecia for funding 50% of the research. This work was supported by the Automotive Mechatronics Chair (a cooperation between Faurecia, CentraleSupélec and Esigelec).

REFERENCES

1. Schelkunoff, S. A., "The impedance concept and its application to problems of reflection, refraction, shielding and power absorption," *Bell System Technical Journal*, Vol. 17, No. 1, 17–48, Jan. 1938.
2. Colaneri, N. F. and L. W. Schacklette, "EMI shielding measurements of conductive polymer blends," *IEEE Transactions on Instrumentation and Measurement*, Vol. 41, No. 2, 291–297, Apr. 1992.
3. Poulichet, P., "Efficacité de blindage des feuilles métalliques," Chapter 2, ESIEE, Paris, Feb. 2004. [Online]. Available: https://perso.esiee.fr/∼poulichp/CEM/Blindage_electromagnetique/chapitre2.PDF.
4. Kühn, M., W. John, and R. Weigel, "Analytical calculation of intrinsic shielding effectiveness for isotropic and anisotropic materials based on measured electrical parameters," *Advances in Radio Science*, Vol. 12, No. C6, 83–89, Nov. 2014.
5. Loya, S. and H. Khan, "Analysis of shielding effectiveness in the electric field and magnetic field and plane wave for infinite sheet metals," *International Journal of Electromagnetics and Applications*, Vol. 6, No. 2, 31–41, Jun. 2016.
6. Moser, J. R., "Low-frequency shielding of a circular loop electromagnetic field source," *IEEE Transactions on Electromagnetic Compatibility*, Vol. 9, No. 1, 6–18, Mar. 1967.
7. Casey, K. F., "Electromagnetic shielding behavior of wire-mesh screens," *IEEE Transactions on Electromagnetic Compatibility*, Vol. 30, No. 3, 298–306, Aug. 1988.
8. Wilson, P. F. and M. T. Ma, "Techniques for measuring the electromagnetic shielding effectiveness of materials. II. Near-field source simulation," *IEEE Transactions on Electromagnetic Compatibility*, Vol. 30, No. 3, 251–259, Aug. 1988.
9. Munalli, D., G. Dimitrakis, D. Chronopoulos, S. Greedy, and A. Long, "Electromagnetic shielding effectiveness of carbon fiber reinforced composites," *Composites Part B: Engineering*, Vol. 173, Sep. 2019.
10. Yang, S., K. Lozano, A. Lomeli, H. D. Foltz, and R. Jones, "Electromagnetic interference shielding effectiveness of carbon nanofiber/LCP composites," *Composites Part A: Applied Science and Manufacturing*, Vol. 36, No. 5, 691–697, May 2005.
11. Wieckowski, T. W. and J. M. Janukiewicz, "Methods for evaluating the shielding effectiveness of textiles," *Fibres & Textiles in Eastern Europe*, Vol. 5, No. 59, 18–22, 2006.
12. Wilson, P. F., M. T. Ma, and J. W. Adams, "Techniques for measuring the electromagnetic shielding effectiveness of materials. I. Far-field source simulation," *IEEE Transactions on Electromagnetic Compatibility*, Vol. 30, No. 3, 239–250, 1988.
13. Chung, D. D. L., "Materials for electromagnetic interference shielding," *Journal of Materials Engineering and Performance*, Vol. 9, No. 3, 350–354, 2000.
14. Criel, S., L. Martens, and D. De Zutter, "Theoretical and experimental near-field characterization of perforated shields," *IEEE Transactions on Electromagnetic Compatibility*, Vol. 36, No. 3, 161–168, 1994.
15. Gooch, J. W. and J. K. Daher, "Fundamentals of electromagnetic shielding," *Electromagnetic Shielding and Corrosion Protection for Aerospace Vehicles*, 1–70, Springer, New York, NY, Mar. 2007.
16. McDowell, A. and T. Hubing, "Decomposition of shielding effectiveness into absorption and reflection components," Tech. Rep., Clemson University, 2014.
17. Al Achkar, G., L. Pichon, M. Bensetti, and L. Daniel, "Homogenization of metal grid reinforced composites for near-field low-frequency magnetic shielding," *Progress In Electromagnetics Research M*, Vol. 99, 153–163, 2020.
18. Andrieu, G., J. Panh, A. Reineix, P. Pélissou, C. Girard, X. Romeuf, and D. Schmitt, "Homogenization of composite panels from a near-field magnetic shielding effectiveness measurement," *IEEE Transactions on Electromagnetic Compatibility*, Vol. 54, No. 3, 700–703, Mar. 2012.